

Cite this: *J. Mater. Chem. A*, 2023, **11**, 15389Received 1st March 2023
Accepted 13th June 2023

DOI: 10.1039/d3ta01259j

rsc.li/materials-a

Thermal properties and phase transition behaviors of possible caloric materials $\text{Bi}_{0.95}\text{Ln}_{0.05}\text{NiO}_3$ [†]

Chen Chen, Yoshihisa Kosugi, Masato Goto and Yuichi Shimakawa

Thermal properties and phase transition behaviors of possible caloric materials $\text{Bi}_{0.95}\text{Ln}_{0.05}\text{NiO}_3$ (Ln = La, Nd, Sm, Eu, Gd, Dy), which show intersite charge transfer between Bi and Ni ions, were investigated. Although a few of the compounds showed large latent heats at the intersite-charge-transfer transition temperatures, the values are not comparable to that observed in the giant caloric effect compound $\text{NdCu}_3\text{Fe}_4\text{O}_{12}$. In the present $\text{Bi}_{0.95}\text{Ln}_{0.05}\text{NiO}_3$, contrary to our expectation, the magnetic transitions of Ni^{2+} spins are not induced by the intersite-charge-transfer transitions and the magnetic entropy changes do not contribute to the latent heat produced by the intersite-charge-transfer transitions. To obtain giant caloric effects, materials for which the "intrinsic" magnetic transition temperatures are much higher than the charge-transfer-transition temperatures may be needed.

Introduction

Refrigeration is an indispensable technology in modern society. However, potent greenhouse gases used by traditional refrigeration increase the global warming potential and thus need to be eliminated for reducing climate change in the future.¹ A solid-state caloric-effect-cooling technology can provide a desirable solution for the problems.^{2,3} The caloric effects of solids usually include magnetocaloric, electrocaloric, and barocaloric effects, in which thermal properties are controlled respectively by applying magnetic fields, electric fields, and pressure.^{4–8} Lots of materials showing caloric effects have been discovered and some such as $\text{La}(\text{Fe}, \text{Si}, \text{Mn})_{13}\text{H}_y$ and Gd alloys have been developed for use in future technology applications.^{8–10}

Recently, a new oxide material $\text{NdCu}_3\text{Fe}_4\text{O}_{12}$ which showed a giant caloric effect was discovered. The compound crystallized in the A-site ordered quadruple perovskite structure, where the Nd^{3+} and Cu^{2+} ions were 1 : 3 ordered at the A site of the simple perovskite structure and the unusually high valence $\text{Fe}^{3.75+}$ ions were located at the center of corner-sharing oxygen octahedra.¹¹ To relieve its electronic instability due to the unusually high valence $\text{Fe}^{3.75+}$ ions, the compound showed an intersite-charge-transfer transition near room temperature.^{12,13} Importantly, a significant latent heat of 25.5 kJ kg^{-1} was provided by the charge-transfer transition and the heat flow can be utilized as a barocaloric effect by applying pressure.¹⁴ An important point in the giant caloric effect of $\text{NdCu}_3\text{Fe}_4\text{O}_{12}$ is that the large entropy change due to simultaneous structural and magnetic transitions

is induced by the charge-transfer transition. A similar large entropy change induced by the charge-disproportionation transition was also found in $\text{BiCu}_3\text{Cr}_4\text{O}_{12}$, where a latent heat of 5.23 kJ kg^{-1} can be utilized by applying both magnetic fields and pressure.¹⁵ In the caloric effects of $\text{NdCu}_3\text{Fe}_4\text{O}_{12}$ and $\text{BiCu}_3\text{Cr}_4\text{O}_{12}$, the charge transitions induced unusual first-order magnetic transitions, and large changes in the magnetic entropies were abruptly yielded at the charge-transition temperatures.¹⁶

These results aroused interest in exploring novel transition-metal oxides showing charge-transfer transitions for solid caloric materials. If we find a compound where the charge-transition induces the first-order magnetic transition, we would have a chance to see a large entropy change, which is utilized as the caloric effect. We then focus on $\text{Bi}_{0.95}\text{La}_{0.05}\text{NiO}_3$, which showed an intersite-charge transfer between the A-site Bi and the B-site Ni described as $0.5\text{Bi}^{3+}\text{--Ni}^{3+} \leftrightarrow 0.5\text{Bi}^{5+}\text{--Ni}^{2+}$. The compound thus changed from the high-temperature $Pnma$ $(\text{Bi}, \text{La})^{3+}\text{Ni}^{3+}\text{O}_3$ phase to the low-temperature $P\bar{1}$ $(\text{Bi}, \text{La})^{3+}_{0.5}\text{Bi}^{5+}_{0.5}\text{Ni}^{2+}\text{O}_3$ phase near room temperature, as shown in Fig. 1.^{17–19} Associated with the transition were observed a negative-thermal-expansion-like large structural change and a ferrimagnetic-like behavior due to canting of antiferromagnetically coupled Ni^{2+} magnetic moments. We thus expected to see a large entropy change similar to those observed in $\text{NdCu}_3\text{Fe}_4\text{O}_{12}$ and $\text{BiCu}_3\text{Cr}_4\text{O}_{12}$.¹⁶ Given that a large latent heat is induced by the charge transition, we will have a chance to see a large barocaloric effect because the charge-transfer transition temperature of $\text{Bi}_{0.95}\text{La}_{0.05}\text{NiO}_3$ changes with changing pressure.²⁰ In addition, $\text{Bi}_{0.95}\text{La}_{0.05}\text{NiO}_3$ was reported to show a ferrimagnetic-like behavior. Thus, the compound may show both barocaloric and magnetocaloric effects like $\text{BiCu}_3\text{Cr}_4\text{O}_{12}$.

In this study, we made a series of $\text{Bi}_{0.95}\text{Ln}_{0.05}\text{NiO}_3$ (Ln = La, Nd, Sm, Eu, Gd, Dy) compounds and investigated their charge

Institute for Chemical Research, Kyoto University, Gokasho, Uji, Kyoto 611-0011, Japan. E-mail: shimak@sci.kyoto-u.ac.jp

[†] Electronic supplementary information (ESI) available: Supporting information is available in the online version of the paper. Correspondence and requests for materials should be addressed to Y. S. See DOI: <https://doi.org/10.1039/d3ta01259j>

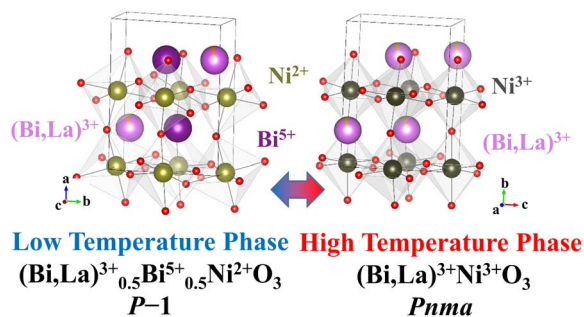


Fig. 1 Schematic illustration of the intersite charge-transfer transition in $\text{Bi}_{0.95}\text{Ln}_{0.05}\text{NiO}_3$. The high-temperature $Pnma$ $(\text{Bi,Ln})^{3+}\text{Ni}^{3+}\text{O}_3$ phase changes to the low-temperature $P\bar{1}$ $(\text{Bi,Ln})^{3+}_{0.5}\text{Bi}^{5+}_{0.5}\text{Ni}^{2+}\text{O}_3$ phase by intersite charge transfer between Bi and Ni ions.

and magnetic transition behaviors. Although the charge and magnetic transitions appeared to occur concomitantly in $\text{Bi}_{0.95}\text{La}_{0.05}\text{NiO}_3$,²⁰ we found that those transitions of $\text{Bi}_{0.95}\text{Ln}_{0.05}\text{NiO}_3$ intrinsically occur separately. As a result, a magnetic entropy change induced by the magnetic transition does not contribute to the entropy change caused by the charge-transfer transition. Details of the transition behaviors will be discussed.

Experiments

$\text{Bi}_{0.95}\text{Ln}_{0.05}\text{NiO}_3$ ($\text{Ln} = \text{La, Nd, Sm, Eu, Gd, Dy}$) samples were synthesized by a solid-state reaction under high-pressure and high-temperature conditions. To prepare the precursors, stoichiometric amounts of Bi_2O_3 , Ln_2O_3 , and Ni raw materials were first dissolved in 6 M nitric acid and the solution was dried by evaporating the acid. The obtained powder samples were then calcined at 973 K for 12 h. Polycrystalline samples of $\text{Bi}_{0.95}\text{Ln}_{0.05}\text{NiO}_3$ were synthesized by treating the precursors under high-pressure (6 GPa) and high-temperature (1273 K) conditions for 30 min in the presence of oxidizer KClO_4 (20 wt% to the precursor). To remove resultant KCl, the synthesized samples were washed with distilled water.

For phase determination, the samples were characterized by X-ray diffraction (XRD) with a BRUKER D8 ADVANCE diffractometer. The $\text{Bi}_{0.95}\text{Nd}_{0.05}\text{NiO}_3$ sample was further characterized by synchrotron X-ray diffraction (SXRD) at SPring-8 (wavelength = 0.50032 Å). The sample was packed into a glass capillary and was kept rotating during data collection. The SXRD data were analyzed by the Rietveld method with the program RIETAN-FP and the crystal structure figures were drawn by using the VESTA software.^{21,22} Magnetic susceptibility of the samples was measured in the range of 5–350 K under a 1 kOe magnetic field with a Quantum Design MPMS3. Heat flow data of the samples in the cooling process were obtained with a NETZSCH DSC3500 at a temperature change rate of 10 K min^{−1}.

Results and discussion

All synthesized samples were confirmed to be nearly single phases with perovskite structures. Although a few peaks, which were not assigned to those of any of the known phases, were

seen in the SXRD patterns, the intensities were very low. The amounts of impurities are thus very little. The samples showed the intersite-charge-transfer transitions, as reported in ref. 19. The transition temperature changes from 430 K for $\text{Bi}_{0.95}\text{Dy}_{0.05}\text{NiO}_3$ to 300 K for $\text{Bi}_{0.95}\text{La}_{0.05}\text{NiO}_3$. Fig. 2 shows an example of the change in the SXRD patterns associated with the intersite-charge-transfer transition seen in $\text{Bi}_{0.95}\text{Nd}_{0.05}\text{NiO}_3$. As in the transition of $\text{Bi}_{0.95}\text{La}_{0.05}\text{NiO}_3$, the orthorhombic $Pnma$ structure observed at 450 K changes to the triclinic $P\bar{1}$ structure at 300 K. The refined structure parameters are given in Tables S1 and S2 in the ESI.† The transition at 360 K accompanies the negative-

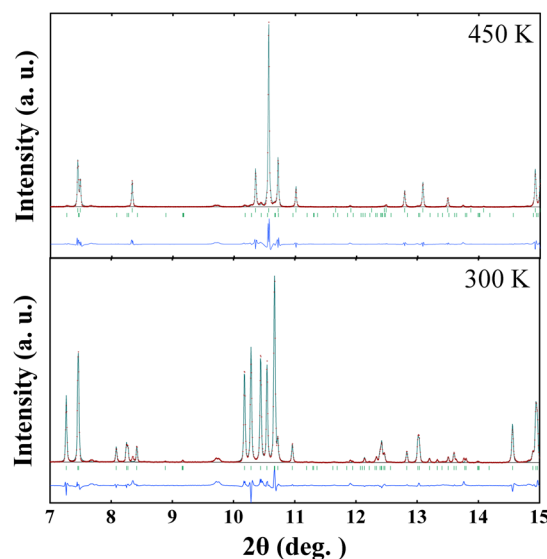


Fig. 2 Results of the Rietveld analysis of the high-temperature (450 K) phase ($R_{\text{wp}} = 11.7\%$) and low-temperature (300 K) phase ($R_{\text{wp}} = 8.9\%$) of $\text{Bi}_{0.95}\text{Nd}_{0.05}\text{NiO}_3$.

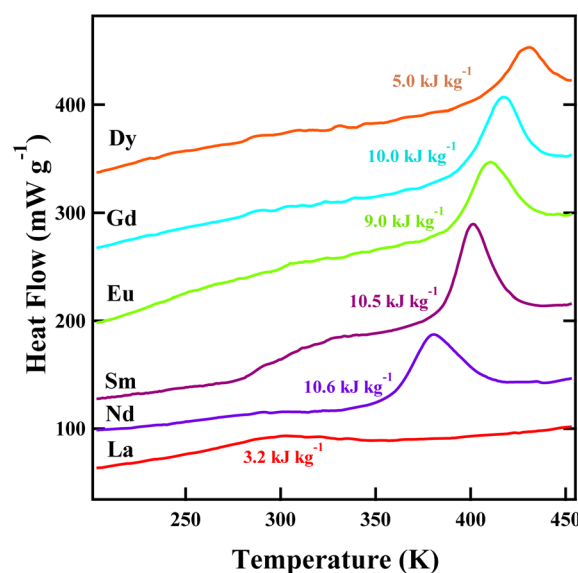


Fig. 3 DSC results for $\text{Bi}_{0.95}\text{Ln}_{0.05}\text{NiO}_3$ ($\text{Ln} = \text{La, Nd, Sm, Eu, Gd, Dy}$) measured on cooling. The observed latent heat is included in the figure. The data for $\text{Ln} = \text{Nd, Sm, Eu, Gd, Dy}$ are plotted with offsets.



thermal-expansion-like volume change, as reported previously.²³ The transition is first-order-like with abrupt changes in the lattice parameters, and the actual transition gives a two-phase coexistence.^{23,24}

Fig. 3 shows the results of differential scanning calorimetry (DSC) measurements for $\text{Bi}_{0.95}\text{Ln}_{0.05}\text{NiO}_3$. Significant latent heats were observed at the intersite-charge-transfer transition temperatures. The values are quite large, but are not comparable to that observed in the giant caloric effect compound $\text{NdCu}_3\text{Fe}_4\text{O}_{12}$.^{11,14} No apparent Ln-dependent relation of the observed latent heat was seen. The heat flow peak for $\text{Bi}_{0.95}\text{La}_{0.05}\text{NiO}_3$ was rather broad and the latent heat was small compared to the other samples.

The observed latent heat produced by the intersite-charge-transfer transition for $\text{Bi}_{0.95}\text{Nd}_{0.05}\text{NiO}_3$ was 10.6 kJ kg^{-1} as shown in Fig. 3 and 4(a) and the corresponding entropy change was estimated to be $27.7 \text{ J K}^{-1} \text{ kg}^{-1}$. In the temperature dependence of magnetic susceptibility of $\text{Bi}_{0.95}\text{Nd}_{0.05}\text{NiO}_3$ shown in Fig. 4(b), on the other hand, we found that the magnetic transition temperature of Ni^{2+} spins was 295 K, which was lower than the intersite-charge-transfer-transition temperature. In the DSC measurement result shown in Fig. 4(a), indeed, a small heat-flow peak was observed at the magnetic transition temperature. Note here that the doped Nd^{3+} magnetic moments show antiferromagnetic-like order at about 14 K (inset

of Fig. 4(b)) and are paramagnetic above that temperature. Besides, no significant structure change was observed at the magnetic transition temperature.²⁴ The results indicate that the magnetic transition of the Ni^{2+} spins is not induced by the intersite-charge-transfer transition of $\text{Bi}_{0.95}\text{Nd}_{0.05}\text{NiO}_3$. This is in sharp contrast to the behavior observed in the intersite-charge-transfer transition in $\text{NdCu}_3\text{Fe}_4\text{O}_{12}$.^{14,16}

Separated charge- and magnetic-transition behaviors were also observed for the samples doped with other Ln ions, and the results are plotted in Fig. 5. The magnetic transition temperatures of the Ni^{2+} spins are lower than the intersite-charge-transfer transition temperatures. With changing the Ln ions from Dy to La increasing the ionic radii, interestingly, the intersite-charge-transfer transition temperature decreases, whereas the magnetic transition temperature looks to be constant. For $\text{Bi}_{0.95}\text{La}_{0.05}\text{NiO}_3$, the intersite-charge-transfer transition temperature seems to coincide with the magnetic transition temperature. The results clearly show that the magnetic transitions are not induced by the intersite-charge-transfer transitions of $\text{Bi}_{0.95}\text{Ln}_{0.05}\text{NiO}_3$, in contrast to the cases of $\text{NdCu}_3\text{Fe}_4\text{O}_{12}$ and $\text{BiCu}_3\text{Cr}_4\text{O}_{12}$. Importantly, the results also imply that the magnetic entropy change does not contribute to the latent heat produced by the intersite-charge-transfer transition. The observed latent heat at the intersite-charge-transfer transition temperature is thus produced only by the charge and lattice entropy changes.

In large caloric effect oxides like $\text{NdCu}_3\text{Fe}_4\text{O}_{12}$ and $\text{BiCu}_3\text{Cr}_4\text{O}_{12}$, the “intrinsic” magnetic transition temperatures are much higher than the charge-transition temperatures. As a result, the magnetic entropy, which intrinsically has to be gradually changed below the magnetic transition temperature according to the second-order transition, is thus abruptly yielded by the very sharp first-order charge (= magnetic) transition.¹⁶ In the present $\text{Bi}_{0.95}\text{Ln}_{0.05}\text{NiO}_3$, in contrast, the magnetic transitions of the Ni^{2+} spins are usual second-order type and the magnetic entropy changes due to the spin order are not so

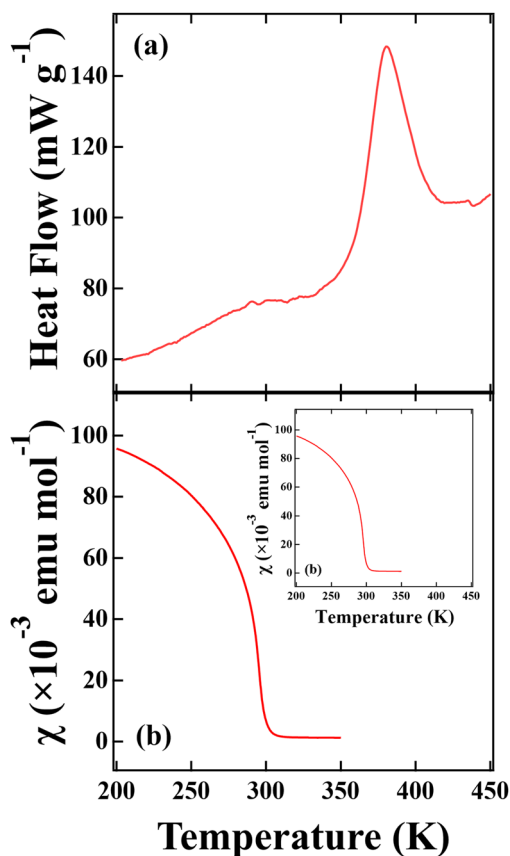


Fig. 4 The DSC curve and magnetic susceptibility of $\text{Bi}_{0.95}\text{Nd}_{0.05}\text{NiO}_3$. The inset shows the magnetic susceptibility at low temperatures, where the antiferromagnetic transition of the Nd^{3+} moment was seen at 14 K.

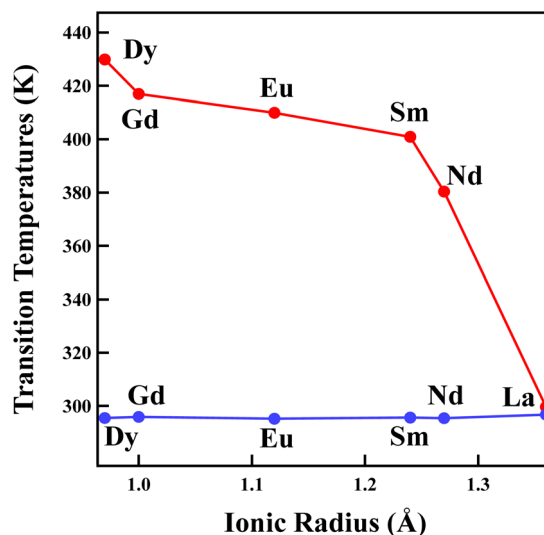


Fig. 5 Intersite-charge-transfer transition (red) and magnetic transition (blue) temperatures of $\text{Bi}_{0.95}\text{Ln}_{0.05}\text{NiO}_3$ (Ln = La, Nd, Sm, Eu, Gd, Dy).



significant, as consistent with the observed small DSC magnetic peaks. The magnetic transition temperatures of $\text{Bi}_{0.95}\text{Ln}_{0.05}\text{NiO}_3$ are determined by superexchange interaction of the Ni^{2+} spins *via* oxygen ions.¹⁷ This explains why the magnetic transition temperatures are nearly the same for all $\text{Bi}_{0.95}\text{Ln}_{0.05}\text{NiO}_3$. An important consequence is that, contrary to our expectation, the giant entropy changes due to the unusual first-order-type magnetic transition like that seen in $\text{NdCu}_3\text{Fe}_4\text{O}_{12}$ cannot be achieved in the present $\text{Bi}_{0.95}\text{Ln}_{0.05}\text{NiO}_3$ system. If the intrinsic magnetic transition temperatures of $\text{Bi}_{0.95}\text{Ln}_{0.05}\text{NiO}_3$ were higher than the intersite-charge-transfer-transition temperatures, we may have a chance to see giant entropy changes, which can be utilized as giant caloric effects.

It is also interesting to note that the obtained phase diagram, in which the charge and magnetic transition temperatures are plotted as a function of the ionic radius of Ln, shows a similarity to that for the metal-insulator and magnetic transitions of LnNiO_3 .^{25,26} The charge-related transition temperatures (the metal-insulator transitions for LnNiO_3 and the intersite-charge-transfer transitions for $\text{Bi}_{0.95}\text{Ln}_{0.05}\text{NiO}_3$) decrease significantly with changing the Ln ion from Lu(Dy) to La, while the magnetic transition temperature is less sensitive to the change. And both transition temperatures become the same for Ln ions with a relatively large ionic radius (La for $\text{Bi}_{0.95}\text{Ln}_{0.05}\text{NiO}_3$ and Sm(Nd) for LnNiO_3).^{25,26} The magnetic transition temperatures for the present $\text{Bi}_{0.95}\text{Ln}_{0.05}\text{NiO}_3$ are around 300 K and are higher than those for LnNiO_3 because the magnetic interaction of Ni^{2+} ($S = 1$) in $\text{Bi}_{0.95}\text{Ln}_{0.05}\text{NiO}_3$ should be strong compared to that of low-spin Ni^{3+} ($S = 1/2$) in LnNiO_3 .

Conclusions

We focused on $\text{Bi}_{0.95}\text{Ln}_{0.05}\text{NiO}_3$ (Ln = La, Nd, Sm, Eu, Gd, Dy), which showed intersite charge transfer between Bi and Ni ions, as possible caloric materials because a similar charge-transition compound $\text{NdCu}_3\text{Fe}_4\text{O}_{12}$ was recently reported to show a giant caloric effect. Importantly, we found from the thermal property measurements that $\text{Bi}_{0.95}\text{Nd}_{0.05}\text{NiO}_3$ provided a significant latent heat of about 10.6 kJ kg^{-1} by the intersite-charge-transfer transition, but the value was not as large as that observed in $\text{NdCu}_3\text{Fe}_4\text{O}_{12}$. This was because the magnetic transition occurred at a temperature lower than the intersite-charge-transfer-transition temperature and the magnetic entropy change did not contribute to the latent heat produced by the intersite-charge-transfer transition. Although the intersite-charge-transfer transition temperature seemed to coincide with the magnetic transition temperature in $\text{Bi}_{0.95}\text{La}_{0.05}\text{NiO}_3$, they were separate in the other series of the compounds. The magnetic transitions of the Ni^{2+} spins in $\text{Bi}_{0.95}\text{Ln}_{0.05}\text{NiO}_3$ were usual second-order type and the magnetic entropy changes due to the spin order were not so significant.

Author contributions

Y. K. and Y. S. conceived the idea and initiated the project. M. G. and Y. S. supervised the project. C. C., Y. K., and M. G. prepared the samples and performed structure analysis as well as

property measurements. All authors discussed the experimental data and wrote the manuscript.

Conflicts of interest

There are no conflicts to declare.

Acknowledgements

We thank S. Kawaguchi and S. Kobayashi for help in synchrotron X-ray diffraction measurements. The synchrotron radiation experiments were performed at the Japan Synchrotron Radiation Research Institute, Japan (proposal No. 2022B1694). This work was partly supported by Grants-in-Aid for Scientific Research (No. 19H05823, 19K15585, 20K20547, 20H00397, 22J15128, 22KK0075, and 23H05457) and by grants for the Integrated Research Consortium on Chemical Sciences and the International Collaborative Research Program of Institute for Chemical Research in Kyoto University from the Ministry of Education, Culture, Sports, Science and Technology (MEXT) of Japan. The work was also partly supported by Japan Science and Technology Agency (JST) as part of Advanced International Collaborative Research Program (AdCORP), Grant Number JPMJKB 2304.

Notes and references

- 1 M. O. McLinden, J. S. Brown, R. Brignoli, A. F. Kazakov and P. A. Domanski, *Nat. Commun.*, 2017, **8**, 14476.
- 2 A. M. Omer, *Renewable Sustainable Energy Rev.*, 2008, **12**, 2265–2300.
- 3 J. M. Calm, *Int. J. Refrig.*, 2008, **31**, 1123–1133.
- 4 A. S. Mischenko, Q. Zhang, J. F. Scott, R. W. Whatmore and N. D. Mathur, *Science*, 2006, **311**, 1270–1271.
- 5 B. Neese, B. Chu, S. G. Lu, Y. Wang, E. Furman and Q. M. Zhang, *Science*, 2008, **321**, 821–823.
- 6 D. Matsunami and A. Fujita, *Appl. Phys. Lett.*, 2015, **106**, 042901.
- 7 L. Mañosa, D. González-Alonso, A. Planes, E. Bonnot, M. Barrio, J. L. Tamarit, S. Aksoy and M. Acet, *Nat. Mater.*, 2010, **9**, 478–481.
- 8 K. Navickaitė, H. N. Bez, T. Lei, A. Barcza, H. Vieyra, C. R. H. Bahl and K. Engelbrecht, *Int. J. Refrig.*, 2018, **86**, 322–330.
- 9 S. Taskaev, V. Khovaylo, D. Karpenkov, I. Radulov, M. Ulyanov, D. Bataev, A. Dyakonov, D. Gunderov, K. Skokov and O. Gutfleisch, *J. Alloys Compd.*, 2018, **754**, 207–214.
- 10 R. Teyber, J. Holladay, K. Meinhardt, E. Polikarpov, E. Thomsen, J. Cui, A. Rowe and J. Barclay, *Appl. Energy*, 2019, **236**, 426–436.
- 11 Y. Shimakawa, *Inorg. Chem.*, 2008, **47**, 8562–8570.
- 12 Y. W. Long, N. Hayashi, T. Saito, M. Azuma, S. Muranaka and Y. Shimakawa, *Nat.*, 2009, **458**, 60–63.
- 13 S. Chakrabarty, S. Bandyopadhyay, A. Dutta and M. Pal, *Mater. Chem. Phys.*, 2019, **233**, 310–318.



- 14 Y. Kosugi, M. Goto, Z. Tan, A. Fujita, T. Saito, T. Kamiyama, W. T. Chen, Y. C. Chuang, H. S. Sheu, D. Kan and Y. Shimakawa, *Adv. Funct. Mater.*, 2021, **31**, 2009476.
- 15 Y. Kosugi, M. Goto, Z. Tan, D. Kan, M. Isobe, K. Yoshii, M. Mizumaki, A. Fujita, H. Takagi and Y. Shimakawa, *Sci. Rep.*, 2021, **11**, 12682.
- 16 Y. Shimakawa and Y. Kosugi, *J. Mater. Chem. A*, 2023, **11**, 12695–12702.
- 17 S. Ishiwata, M. Azuma, M. Takano, E. Nishibori, M. Takata, M. Sakata and K. Kato, *J. Mater. Chem.*, 2002, **12**, 3733–3737.
- 18 M. Azuma, S. Carlsson, J. Rodgers, M. G. Tucker, M. Tsujimoto, S. Ishiwata, S. Isoda, Y. Shimakawa, M. Takano and J. P. Attfield, *J. Am. Chem. Soc.*, 2007, **129**, 14433–14436.
- 19 K. Oka, M. Mizumaki, C. Sakaguchi, A. Sinclair, C. Ritter, J. P. Attfield and M. Azuma, *Phys. Rev. B*, 2013, **88**, 014112.
- 20 S. Ishiwata, M. Azuma, M. Hanawa, Y. Moritomo, Y. Ohishi, K. Kato, M. Takata, E. Nishibori, M. Sakata, I. Terasaki and M. Takano, *Phys. Rev. B*, 2005, **72**, 045104.
- 21 H. M. Rietveld, *J. Appl. Crystallogr.*, 1969, **2**, 65–71.
- 22 F. Izumi and K. Momma, *Solid State Phenom.*, 2007, **130**, 15–20.
- 23 M. Azuma, W. T. Chen, H. Seki, M. Czapski, S. Olga, K. Oka, M. Mizumaki, T. Watanuki, N. Ishimatsu, N. Kawamura, S. Ishiwata, M. G. Tucker, Y. Shimakawa and J. P. Attfield, *Nat. Commun.*, 2011, **2**, 347.
- 24 K. Oka, K. Nabetani, C. Sakaguchi, H. Seki, M. Czapski, Y. Shimakawa and M. Azuma, *Appl. Phys. Lett.*, 2013, **103**, 061909.
- 25 J. B. Torrance, P. Lacorre, A. I. Nazzari, E. J. Ansaldo and C. Niedermayer, *Phys. Rev. B*, 1992, **45**, 8209.
- 26 J. S. Zhou, J. B. Goodenough, B. Dabrowski, P. W. Klamut and Z. Bukowski, *Phys. Rev. Lett.*, 2000, **84**, 526.

